

SINGLE-PHASE LEVEL SET METHOD FOR UNSTEADY VISCOUS FREE SURFACE FLOWS

Pablo M. Carrica^{*}, Robert V. Wilson^{*}, Frederick Stern^{*}

^{*} IIHR-Hydroscience and Engineering

The University of Iowa

300 Riverside Dr.

Iowa City, IA 52242-1585

e-mail: pablo-carrica@uiowa.edu, web page: <http://iihr.uiowa.edu>

Key words: free surface, incompressible viscous flows, single-phase level set, unsteady.

Abstract. *The level-set method has become a popular approach to tackle two-phase, incompressible flow problems. In the standard level-set method the equations are solved in both fluids with smoothed fluid properties across the interface. In contrast to the standard level set method, the single-phase level set method is concerned with the solution of the flow field in the denser phase only. Some of the advantages of such an approach are that the interface remains sharp, the computation is performed within a fluid with uniform properties and that only minor computations are needed in the air. The location of the interface is determined using a signed distance function, exactly as done on the standard level-set method, but appropriate interpolations and extrapolations are used at the fluid/fluid interface to enforce the jump conditions. In our RANS solver with non-orthogonal grids, very large cell aspect ratios appear on the near-wall regions of the flow, which causes the standard reinitialization methods to fail. To overcome this problem, a reinitialization procedure has been developed that works well with non-orthogonal grids with large aspect ratios. Since the grid points in air don't have a well defined velocity, the time derivatives cannot be treated in the Eulerian fashion in points that change from air to water during a time step. This problem is dealt with by using a convective extension to obtain the velocities at previous time-steps for the grid points in air, which provides a good estimation of the total derivatives. In this paper we discuss the details of such implementations. The method was applied to two unsteady tests: sloshing in a two-dimensional tank and wave diffraction in a surface ship, and the results compared against analytical solutions or experimental data. The method can in principle be applied to any problem in which the standard level-set method works, as long as the stress on the second phase can be specified and no bubbles appear in the flow during the computation.*

1 INTRODUCTION

Level set methods are becoming increasingly popular for the solution of fluid problems involving moving interfaces¹. In the case of fluid/fluid interfaces, the level set methods can predict the evolution of complex free surface topologies including waves with large slopes such as spilling and breaking waves, deforming bubbles and droplets, breakup and coalescence, etc. Initially introduced by Osher & Sethian², the level set method has been the subject of much research and was used to solve different types of problems; see for instance the cited review by Sethian & Smereka¹ and the work by Osher & Fedkiw³.

In many fluid/fluid problems the interface between the fluids can be considered as a free-boundary, which allows for the computation of the flow on the more viscous and dense fluid only. A most important set of problems of this class is the water flow around surface-piercing bodies (like ship hulls) and around submerged bodies (as the flow past a submerged hydrofoil). Most interface tracking methods solve free-boundary problems with appropriate conditions at the interface. Volume of Fluid (VOF) methods solving only the denser phase are common⁴.

Solving only the water phase in level set methods (here called the single-phase level set method) presents several advantages over the classic level set approach (or two-phase level set method) in which both fluids are solved. One of them is that in the air phase only extension velocities are needed, which makes the problem considerably easier to converge. In addition, since we are solving on a single fluid with constant properties, the computation of the pressure can be done in a standard way without pressure and velocity oscillations at the interface that are common in two-phase level set methods with large density ratios. Single-phase level-set method can in principle handle any problem that can be solved with two-phase level-set methods, as long as two conditions are met. The first condition arises from the fact that in single-phase level set methods (or any other method in which we solve only the water phase) the continuity condition will not be satisfied on the air phase, thus the method is not suitable for problems in which the air phase somehow gets pressurized during the computation. This means that the method will yield non-physical results if air is trapped or bubbles are formed inside the liquid during the calculation. The second condition, related to the first, is that the stresses caused on the liquid phase by the air phase must be negligible since, again, we don't compute in the air and impose those stresses to be known *a priori*. Other than these limitations, the method has no restrictions on surface topology.

The main application we pursue in our research program is the computation of the viscous free surface flow in large surface-piercing bodies. This is a difficult problem that involves complicated three-dimensional geometries, which leads to non-orthogonal curvilinear grids with high aspect ratio, very high Reynolds numbers and complex free surface topologies. Both surface tracking and surface capturing methods have been used to tackle this type of problems.

In surface tracking methods, the computational grid is fitted to the free surface, and therefore is not fixed in time. This type of method can be high order accurate both in space and time. The grid deformation process to fit the grid to the free surface works well and is robust as long as the free surface deformation remains small. Examples of successful

applications for free surface ship flows include resistance computation without⁵ and with propellers⁶, forward speed diffraction^{7,8}, roll decay motion⁹ and pitching and heaving motion in regular head seas¹⁰. Unfortunately, as the deformation of the free surface increases it is difficult to prevent grid quality deterioration and computation breakdown. One of the main conclusions drawn after the Gothenburg 2000 workshop on ship hydrodynamics¹¹ was that level-set methods show promising results and further research for surface capturing methods should be pursued to overcome the limitations of surface-tracking methods.

Besides level set methods, surface capturing methods include volume of fluid (VOF) methods¹², front tracking methods¹³, and other variations in which a color or volume fraction function is computed. Among others, notable examples of the application of surface capturing methods for flows around floating bodies are in Azcueta *et al.*¹⁴, where a surface capturing method is used to simulate the flow around a surface piercing blunt body, and in Sato *et al.*¹⁵, who studied pitching and heaving on linear incident waves.

Level set methods have been applied for both submerged and surface-piercing body problems. Both single and two-phase level set methods have been used¹⁶ to study the flow around submerged two-dimensional hydrofoil in steady-state. Complicated three-dimensional flows around container ships using the two-phase level set approach with body-fitted coordinates have been solved^{17,18,19}. Three-dimensional flows around ships have been tackled in steady-state using a single-phase level set method²⁰. We note that all these single-phase methods are devised and used for steady-state applications only.

In this paper we present an unsteady single-phase level set method for viscous, incompressible flow. The computation of the total time derivative is a key issue to make the method time-accurate. The implementation of the overall scheme is discussed.

We test the method against two two-dimensional and one three-dimensional unsteady cases: a linear progressive wave, the sloshing in a steady tank, and the wave diffraction by a ship. Results are compared against analytical or experimental data showing good agreement.

2 LEVEL SET APPROACH

We discuss first the standard level set method for incompressible free surface viscous flows, originated about ten years ago²¹. We call this method the two-phase level set, since the solution is obtained in both fluids. In a two-phase flow, the instantaneous local equations of motion within each fluid can be written as²²:

$$\frac{\partial \mathbf{v}_k}{\partial t} + \mathbf{v}_k \cdot \nabla \mathbf{v}_k = -\frac{1}{\rho_k} \nabla p_k + 2 \frac{\mu_k}{\rho_k} \nabla \cdot \mathbf{D}_k + \mathbf{g} \quad (1)$$

$$\nabla \cdot \mathbf{v}_k = 0 \quad (2)$$

where the subscript $k = l$ or g indicates the phase present at a given point in space, which in our case can be either liquid or gas. \mathbf{v} , p and \mathbf{D} are the velocity, pressure and rate of deformation tensor, ρ_k and μ_k are the density and viscosity of fluid k , and \mathbf{g} is the gravity

acceleration. At the interface, the interfacial boundary conditions or jump conditions apply. In the case of immiscible fluids we can write:

$$[-p\mathbf{I} + 2\mu\mathbf{D}] \cdot \mathbf{n} = -(\sigma\kappa\mathbf{n} + \nabla_i\sigma) \quad (3)$$

where the bracket means $l - g$ and the normal \mathbf{n} is taken from the liquid to the gas. The second term on the right hand side of Eq. (3) is the stress due to gradients on surface tension or Marangoni effect²³, usually important when large gradients of temperature are present, as in boiling flow. ∇_i denotes the gradient in the local free surface coordinates. The interfacial curvature κ is computed from:

$$\kappa = \nabla \cdot \mathbf{n} \quad (4)$$

The jump conditions (3) can be integrated into the equations of motion (1) and (2), resulting in a body force concentrated in the interface of a single incompressible fluid with variable properties²⁴:

$$\frac{\partial \mathbf{v}}{\partial t} + \mathbf{v} \cdot \nabla \mathbf{v} = -\frac{1}{\rho} \nabla p + 2\frac{\mu}{\rho} \nabla \cdot \mathbf{D} + \mathbf{g} + (\sigma\kappa\mathbf{n} + \nabla_i\sigma) \delta(\phi) \quad (5)$$

where ϕ is a distance to the interface function, positive in liquid and negative in gas. The location of the interface is therefore the zero level set of the function ϕ , known as the level set function. Since the free surface is a material interface (in absence of interfacial mass transfer such as evaporation or condensation), then the equation for the level set function is:

$$\frac{\partial \phi}{\partial t} + \mathbf{v} \cdot \nabla \phi = 0 \quad (6)$$

and from the level set function we can compute the normal as:

$$\mathbf{n} = -\frac{\nabla \phi}{|\nabla \phi|} \quad (7)$$

Since the fluid properties in Eq. (5) change discontinuously across the interface, and the concentrated surface tension force also becomes infinite in an infinitesimal volume, direct solution of Eq. (5) is naturally difficult. Two approaches are usually followed to overcome these difficulties.

In standard level set methods, the interface is smoothed across a finite thickness region, usually a few grid points thick. The fluid properties and the delta function are modified as²⁰:

$$\rho(\phi) = \rho_g + (\rho_l - \rho_g)H(\phi) \quad (8)$$

$$\mu(\phi) = \mu_g + (\mu_l - \mu_g)H(\phi) \quad (9)$$

$$\delta(\phi) = \frac{dH(\phi)}{d\phi} \quad (10)$$

where the smoothed Heaviside function is usually expressed as:

$$H(\phi) = \begin{cases} 0 & (\phi < -\alpha) \\ 0.5[1 + \phi/\alpha + \sin(\pi\phi/\alpha)/\pi] & (|\phi| \leq \alpha) \\ 1 & (\phi > \alpha) \end{cases} \quad (11)$$

with α the half-thickness of the properties transition region. An important step is to maintain the level set function a distance function within the transition region at all times. This is achieved by the reinitialization step, discussed later in this paper.

One drawback of the level set method is the introduction of the transition region. This results in smearing of the flow properties and variables, forcing them to be continuous at the interface regardless of the appropriate jump conditions. In the Ghost Fluid Method the jump conditions are introduced implicitly on the formulation by solving for a “ghost” fluid across the interface^{25,26}. This approach, though easy to implement, forces the solution of two fluid fields on each grid node, one for each fluid. This results in additional computational cost that can be very demanding in large 3-D computations.

It is then desirable for many applications to be able to solve a single-phase problem in a fixed grid, capturing the interface with appropriate enforcement of the jump conditions, and still retaining the advantages of level set methods. These applications generally involve air-water flows in which the density and viscosity ratios are about 1000 and 75, respectively. Under these conditions, the interface can be taken as shear stress free for most applications, as frequently done with interface tracking algorithms. In this way the computational domain to solve the RANS equations is restricted to the grid points in water plus a few nodes in air to enforce the jump conditions, with the consequent economy of resources. A second advantage is that the continuity equation is enforced always in a single fluid, thus allowing the use of standard collocated methods without the usual pressure and velocity oscillations that occur at the interface between fluids with a large density ratio^{1, p. 355}. Such a method is the single-phase level set method^{16,20}. In this paper we discuss how to compute time derivatives at the interface on a single-phase level set method in order to make it appropriate for unsteady problems.

3 UNSTEADY SINGLE-PHASE LEVEL SET METHOD DETAILS

The key points of a single-phase level-set method are the derivation and implementation of the jump conditions, the reinitialization of the level-set as a distance function and the computation of the total time derivatives. Discussion on these subjects follows.

3.1 Dimensionless equations

Since we work on a single fluid, the RANS equations can be non-dimensionalized as usual:

$$\frac{\partial \mathbf{v}}{\partial t} + \mathbf{v} \cdot \nabla \mathbf{v} = -\nabla p + \nabla \cdot \left(\frac{1}{\text{Re}_{eff}} \nabla \mathbf{v} \right) + \mathbf{S} \quad (12)$$

where \mathbf{S} includes any volumetric source with the exception of the gravity, which is lumped with the pressure to define the non-dimensional piezometric pressure:

$$p = \frac{p_{abs}}{\rho U_0^2} + \frac{z}{Fr^2} \quad (13)$$

In Eqs. (12) and (13) p_{abs} is the absolute pressure, Re_{eff} is the effective Reynolds number and Fr is the Froude number, defined as:

$$\text{Re}_{eff} = \frac{U_0 L}{\nu + \nu_t} \quad (14)$$

$$Fr = \frac{U_0}{\sqrt{gL}} \quad (15)$$

where U_0 is the free-stream velocity and L is the characteristic length. ν_t is the turbulent viscosity, that in our approach, is obtained after solving the blended $k-\omega$ model of turbulence²⁷. Since we are considering an incompressible fluid, the continuity equation reads:

$$\nabla \cdot \mathbf{v} = 0 \quad (16)$$

To capture the location of the interface, we solve the level set function, Eq. (6).

3.2 Jump conditions

In a single-phase level set approach the jump conditions at the interface between two fluids, Eq. (3), must be treated as a boundary condition enforced explicitly. The jump condition on any direction tangential to the free surface is²⁵:

$$\left[\mu(\nabla \mathbf{v} \cdot \mathbf{n}) \cdot \mathbf{t} + \mu(\nabla \mathbf{v} \cdot \mathbf{t}) \cdot \mathbf{n} \right] = 0 \quad (17)$$

Neglecting the viscosity in air, and since \mathbf{t} is an arbitrary vector perpendicular to the normal to the interface, we obtain the boundary conditions for the velocity at the interface:

$$\nabla \mathbf{v} \cdot \mathbf{n} = 0 \quad (18)$$

Normal to the interface, the jump condition in dimensional form can be written as:

$$\left[p_{abs} - 2\mu(\nabla \mathbf{v} \cdot \mathbf{n}) \cdot \mathbf{n} \right] = \sigma \kappa + \nabla_i \sigma \cdot \mathbf{n} \quad (19)$$

In water/air interfaces we can approximate the pressure as constant in the air. Also, because of Eq. (18), the second term on the left hand side of Eq. (19) is zero. Thus the jump condition reduces to:

$$p_{abs} = \sigma\kappa + \nabla_i \sigma \cdot \mathbf{n} \quad (20)$$

We also choose at this point to neglect the surface tension effects, because for the class of problems in which we are interested the curvature of the free surface is small. This is not a limitation of the model and surface tension can be easily included, as done by Di Mascio *et al.*²⁰. Introducing Eq. (13), we must impose at the fluid/fluid interface:

$$p = \frac{z}{Fr^2} \quad (21)$$

3.3 Pressure condition at the free surface

In a surface capturing approach the free surface is not located at the grid points and therefore an interpolation scheme must be devised to enforce the interfacial pressure condition at the interface location, Eq. (21). The free surface itself can be easily identified by locating the change in sign of ϕ between two contiguous grid points along any coordinate line.

We have then in our method three types of grid points. Grid points in water with all the first neighbors in water will be computed without any special treatment and need no additional consideration. Grid points in air can have any pressure value, and then we choose to enforce there Eq. (21) where z is now the vertical coordinate at the point. For points in water in which at least one of the neighbors is in air the following discussion applies.

For any grid point p in water that has a neighbor in air n_a , the interfacial pressure condition of Eq. (21) is enforced locally. Referring to Fig. 1, the relative distance between the grid point in water and the interface is:

$$\eta = \frac{\phi_p}{\phi_p - \phi_{n_a}} \quad (22)$$

thus, interpolating along the line joining the points p and n_a and using Eq. (21) we obtain for the interfacial pressure:

$$p_{int} = \frac{(1-\eta)z_p + \eta z_{n_a}}{Fr^2} \quad (23)$$

The pressure at the neighbor in air can then be found by extrapolation from the pressure values at the points h and at the interface, where h is located halfway between the local point p and the opposite neighbor in water to n_a , shown as n_w in Fig. 1:

$$p_{n_a} = (p_{int} - p_h) \frac{dist(\mathbf{r}_{n_a}, int)}{dist(\mathbf{r}_p, int) + dist(\mathbf{r}_p, \mathbf{r}_h)} + p_{int} \quad (24)$$

where $p_h = (p_p + p_{n_w})/2$ and $\mathbf{r}_h = (\mathbf{r}_p + \mathbf{r}_{n_w})/2$. This scheme can be easily implemented on a subroutine that computes the matrix coefficients for the pressure Poisson equation, by plugging Eq. (24) on every neighbor in air. Since all the necessary neighbors to enforce the

interfacial pressure condition are the same necessary to build the pressure matrix (for typical 19 point stencils), no additional connectivity has been added and therefore can be implemented in multi-block codes with no modifications on the existing inter-block information transfer scheme. This is especially attractive in parallel implementations.

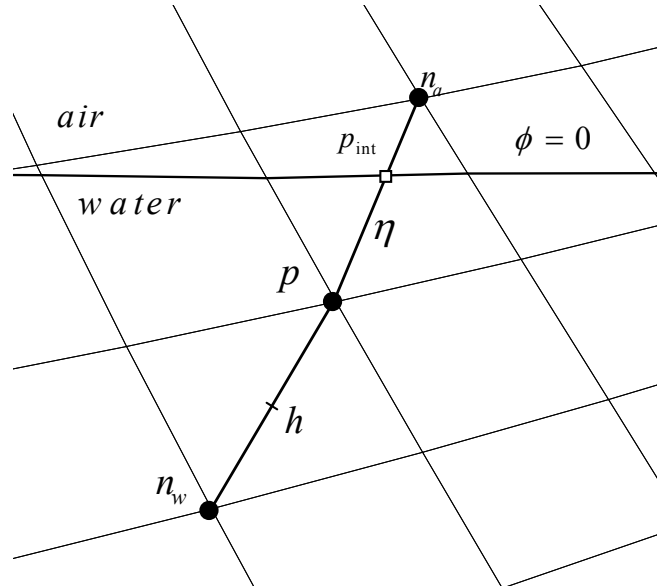


Figure 1: calculation of the neighbor pressure to enforce the pressure boundary condition.

3.4 Reinitialization

In two-phase level set methods, the distance function is reinitialized periodically to keep it a smooth distance function and have a transition region uniform in thickness. The reinitialization step is extremely important in single-phase level set methods but for different reasons: the normal must be accurately evaluated at the interface because it is used in the boundary conditions and it must also be reasonable everywhere in air since it is used to extend the velocities into the air to transport the level set function. The reinitialization step is thoroughly described by Carrica *et al.*²⁸, and will be summarized here.

We extend the method of Adalsteinsson & Sethian²⁹ to three dimensional curvilinear grids to obtain a good signed distance for the first neighbors to an interface (the beginning set of their *close* points). In curvilinear grids with very large aspect ratio (in boundary layer grids can be as large as 10^5) we cannot use the distance to the first neighbor to define the geometrical distance to the interface. In very large aspect ratios the closest interface might lie several grid points away in some direction. Moreover, the closest interface might be in a different block, and thus that information belongs to a different processor in a typical domain decomposition parallel implementation. To account for this problem we search along the three grid lines for an interface, including higher-order neighbors. Once the close-point reinitialization is performed, we solve the implicit equation:

$$\mathbf{n} \cdot \nabla \phi = \text{sign}(\phi_0) \quad (25)$$

where \mathbf{n} is in this case the normal pointing to the fluid being reinitialized. Since \mathbf{n} is either $\nabla \phi$ or $-\nabla \phi$, Eq. (25) is an eikonal equation and propagates information from the interface outwards. The corresponding Dirichlet boundary conditions for (25) are given by the value of ϕ at the close points.

3.5 Computing the total time derivatives

The proper computation of the total time derivative terms near the interface is a problem in single-phase level set techniques. To understand this, consider an interface moving vertically, as shown in Fig. 2, where we want to compute the total derivative at point p . At the current time shown, the point p is in water and in the previous time step was in air. Since we are using an Eulerian approach, the local time derivative at point p is expressed as a first-order approximation as:

$$\frac{\partial \varphi}{\partial t} \cong \frac{\varphi_t - \varphi_{t-\Delta t}}{\Delta t} \quad (26)$$

where φ is any velocity or turbulence variable. The problem appears because $\varphi_{t-\Delta t}$ was in air on the previous time step and therefore its value does not satisfy the field equations since it was computed using the extension of Eq. (18). Previous authors^{16,20} recognize this limitation and deal with steady-state problems only. Notice that in the standard two-phase level set method we can have a problem of similar origin. We use for our analysis the velocities, though all the variables should be computed across the interface on the same way.

In single-phase level set approaches we have a sharp interface, and thus we have to find a suitable velocity for the previous time-steps to assign to the grid point previously in air. One possibility is to use the extended velocity as the previous time-step velocity (or time steps in a higher order scheme). However, this extended velocity will not result in the right total derivative. An extension that will yield a good approximation of the total derivative is presented below.

Let's consider a particle belonging to the free surface that at time $t - \Delta t'$ during the time step advancing from $t - \Delta t$ to t crosses a grid point, marked as p in Fig. 3. From $t - \Delta t'$ to t , the total derivative of the velocity is:

$$\left. \frac{D \mathbf{u}}{Dt} \right|_1 = \frac{\mathbf{u}(\mathbf{r}_p, t - \Delta t') - \mathbf{u}_{t-\Delta t}^{\text{int}}}{\Delta t - \Delta t'} \quad (27)$$

where $\mathbf{u}(\mathbf{r}_p, t - \Delta t')$ is the velocity of the particle on the interface that at $t - \Delta t'$ is exactly on grid point p , and $\mathbf{u}_{t-\Delta t}^{\text{int}}$ is the velocity of the same particle at $t - \Delta t$. This is a Lagrangian evaluation of the acceleration.

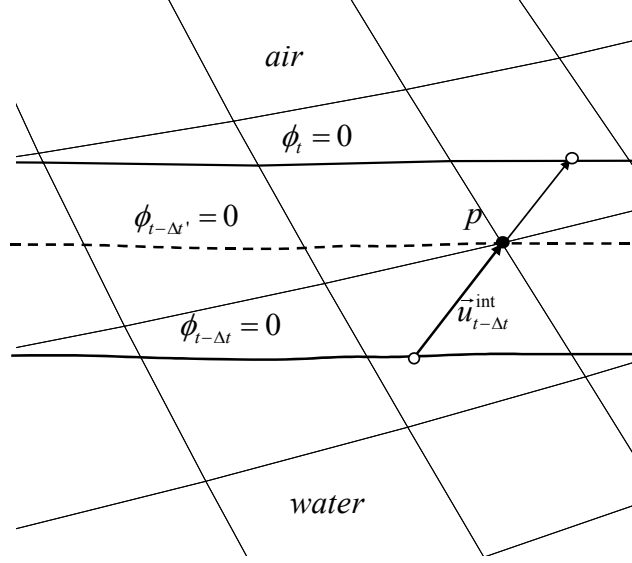


Figure 2: computation of the time derivative at a grid point that is changing fluid.

From $t - \Delta t'$ to t we can use the Eulerian acceleration, since from that time on the grid point p is in water:

$$\left. \frac{D\mathbf{u}}{Dt} \right|_2 = \frac{\mathbf{u}(\mathbf{r}_p, t) - \mathbf{u}(\mathbf{r}_p, t - \Delta t')}{\Delta t'} + \mathbf{u}(\mathbf{r}_p, t) \cdot \nabla \mathbf{u}(\mathbf{r}_p, t) \quad (28)$$

Since both total derivatives are computed within the same time step advancing from $t - \Delta t$ to t , we set $\left. \frac{D\mathbf{u}}{Dt} \right|_1 = \left. \frac{D\mathbf{u}}{Dt} \right|_2$ and solve for the unknown velocity $\mathbf{u}(\mathbf{r}_p, t - \Delta t')$ to obtain:

$$\frac{D\mathbf{u}}{Dt} = \frac{\mathbf{u}(\mathbf{r}_p, t) - \mathbf{u}_{t-\Delta t}^{\text{int}}}{\Delta t} + \frac{\Delta t'}{\Delta t} \mathbf{u}(\mathbf{r}_p, t) \cdot \nabla \mathbf{u}(\mathbf{r}_p, t) \quad (29)$$

Notice that the ratio $\Delta t'/\Delta t$ can be computed from the level set function as:

$$\frac{\Delta t'}{\Delta t} = \frac{\phi(\mathbf{r}_p, t)}{\phi(\mathbf{r}_p, t) - \phi(\mathbf{r}_p, t - \Delta t)} \quad (30)$$

Thus, accordingly to Eqs. (29) and (30), the total time derivative in grid points in which the level set function changes from air to water is replaced by:

$$\frac{D\mathbf{u}}{Dt} = \frac{\mathbf{u}(\mathbf{r}_p, t) - \mathbf{u}_{t-\Delta t}^{\text{int}}}{\Delta t} + \frac{\phi(\mathbf{r}_p, t)}{\phi(\mathbf{r}_p, t) - \phi(\mathbf{r}_p, t - \Delta t)} \mathbf{u}(\mathbf{r}_p, t) \cdot \nabla \mathbf{u}(\mathbf{r}_p, t) \quad (31)$$

where the interfacial particle velocity at $t - \Delta t$, $\mathbf{u}_{t-\Delta t}^{\text{int}}$, remains to be determined. Notice that if

in Eq. (31) we replace this velocity by the velocity at point p on the previous time step we obtain the following expression:

$$\frac{D\mathbf{u}}{Dt} = \frac{\mathbf{u}(\mathbf{r}_p, t) - \mathbf{u}(\mathbf{r}_p, t - \Delta t)}{\Delta t} + \frac{\phi(\mathbf{r}_p, t)}{\phi(\mathbf{r}_p, t) - \phi(\mathbf{r}_p, t - \Delta t)} \mathbf{u}(\mathbf{r}_p, t) \cdot \nabla \mathbf{u}(\mathbf{r}_p, t) \quad (32)$$

The implementation of Eq. (32) requires an easy modification to the convective term and that we load on the points in air the interfacial velocity of the particle that will pass through grid point p , and assign that to the previous time step velocity. This second step is achieved by simply extending the variables not with the normal but with the velocity itself:

$$\mathbf{u}(\mathbf{r}_p, t - \Delta t) \cdot \nabla \mathbf{u}(\mathbf{r}_p, t - \Delta t) = 0 \quad (33)$$

which performs convective extension, thus assigning the interfacial velocity properly. We should be aware that Eq. (33) does not satisfy the normal zero gradient boundary conditions, and thus all the extensions in air during a given time-step must be carried out using Eq. (18). Once the time-step is converged, the extension of Eq. (33) is performed and loaded, only in air, as the previous time-step velocity.

4 IMPLEMENTATION

The single-phase level set model was implemented in the code CFDSHIP-IOWA³⁰, a parallel unsteady RANS code. The code uses body-fitted structured multi-block grids with ghost cells and chimera interpolations to accommodate complex geometries. Thorough discussion of the status and methods used on the code can be found in Wilson *et al.*³¹.

5 NUMERICAL EXAMPLES

Since the aim of this paper is an unsteady method, we concentrate in unsteady example problems. The method has been tested on steady-state three-dimensional problems, including the flow around a surface ship model DTMB 5415 for different Froude numbers³¹.

The numerical method described in the previous sections has been applied to two unsteady cases: sloshing in a 2-D tank and a 3-D wave diffraction problem for a surface combatant.

5.1 Viscous wave in a 2-D tank

We consider a tank with a length that is twice the depth of the still water level, in which a viscous fluid is allowed to oscillate freely. The grid is comprised of 4 blocks each with 51x46 grid points in the x and z directions respectively and the extents are $x \in (-1, 1)$ and $z \in (-1, 0.1)$. At $t = 0$ the free surface has a sinusoidal profile of small amplitude ζ_0 and wavelength $2d$, which in our case is represented by:

$$\zeta_0(x) = 1 - 0.01 \sin\left(\frac{\pi x}{2}\right) \quad (34)$$

The free surface is then released and the wave elevation shows an amplitude decay in time $\zeta(x,t)$. In order to simulate an infinite wave, we impose slip conditions at the lateral walls and at the bottom of the computational domain. Since the velocities are very small at the bottom, the boundary condition there has very little effect.

This problem was studied analytically by Wu *et al.*³², who solved the linearized Navier-Stokes equations. The solutions are expressed for different (small) Reynolds numbers ($Re = d\sqrt{gd}/\nu$) as a function of a dimensionless time expressed as $\tau = t\sqrt{g/d}$. In our method we obtain the same non-dimensionalization by setting $Fr = 1$ and using the same initial amplitude as in the analytical problem. In addition, Eatock Taylor *et al.*³³ provide numerical solutions to this problem using a Pseudo-Spectral Matrix Element Method, which is deemed to be very accurate, though the authors use linearized free surface conditions.

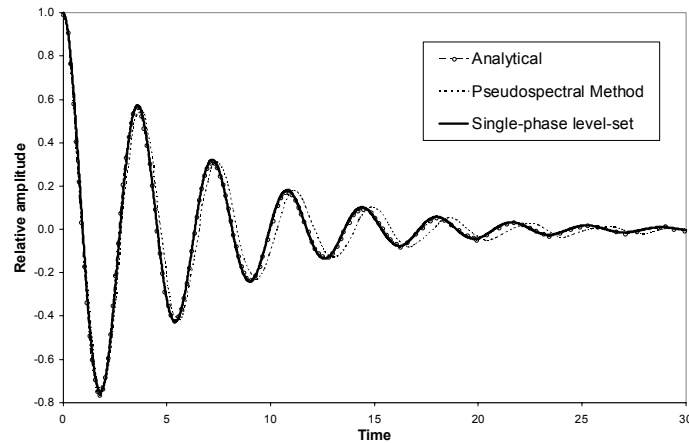


Figure 3: wave amplitude evolution at the center in a two-dimensional tank (Re=100)

To evaluate quantitatively the performance of our numerical method, we compare against the analytical and the pseudo-spectral method solutions³³ at Re=100 in Fig. 3. We see that the single-phase method does an excellent job in predicting both the amplitude and phase of the analytical solution outperforming the pseudo spectral method predictions.

A higher Reynolds number solution (Re=2000) is shown in Fig. 4, compared against the analytical solution³². In this case, the single-phase level set method shows slight phase and amplitude differences. We note that the analytical solution neglects the nonlinear terms in the Navier-Stokes equations and uses a linearized free surface boundary condition, which might lead to error at this Reynolds number. This error, however, has not been quantified.

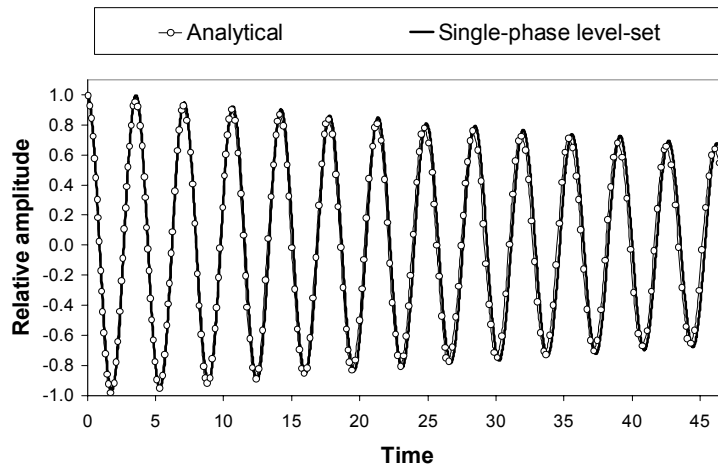


Figure 4: wave amplitude evolution at the center in a two-dimensional tank ($Re=2000$)

5.2 Forward speed diffraction on a surface ship

This problem is attractive as a benchmark because it involves considerable complications with respect to the previous case. Consider a ship moving with constant speed in the presence of regular head waves, that is, the ship and the waves move in opposite directions. Wilson & Stern⁷ and Rhee & Stern⁸ have performed numerical simulations of this problem using surface-tracking methods, Cura Hochbaum & Vogt¹⁹ have used the standard level set method.

This case has been experimentally studied for a DTMB 5512 model. Unsteady free surface elevation, resistance, heave force and pitch moments^{34,35} and velocities³⁶ were measured. Free surface elevations and velocities were measured only at medium Froude number ($Fr = 0.28$), long wavelength ($\lambda = 1.5L$) and low wave steepness ($Ak = 0.025$). Thus, these conditions were selected for comparison with the numerical method. Since the model ship has a length $L = 3.048m$, a Froude number $Fr = 0.28$ corresponds to $Re = 4.65 \cdot 10^6$.

In order to simulate the boundary layer turbulence using the $k-\omega$ model, a fine near wall discretization is necessary, with spacing around $10^{-6}L$. This makes the design of the computational grid difficult, since an orthogonal grid is convenient in the far field to avoid deformation of the incoming wave. This problem can be overcome using a body-fitted grid for the boundary layer and an orthogonal grid for the far-field using overset grids with Chimera³⁷ interpolation. In our case we chose to use an 8 block boundary layer body-fitted grid, a 16 block close-field orthogonal grid and a 8 block far-field orthogonal grid, for a total of 32 blocks and approximately 2,000,000 grid points. The overall grid, shown in Fig. 5, extends from $x = -1$ to $x = 2$, $y \in (0, 1)$, taking advantage of the symmetry of the problem about the centerplane $y = 0$, and $z \in (-1, 0.1)$, with the ship located between $x = 0$ to $x = 1$. Ghost cells were used for interblock coupling inside each of the three main grid systems.

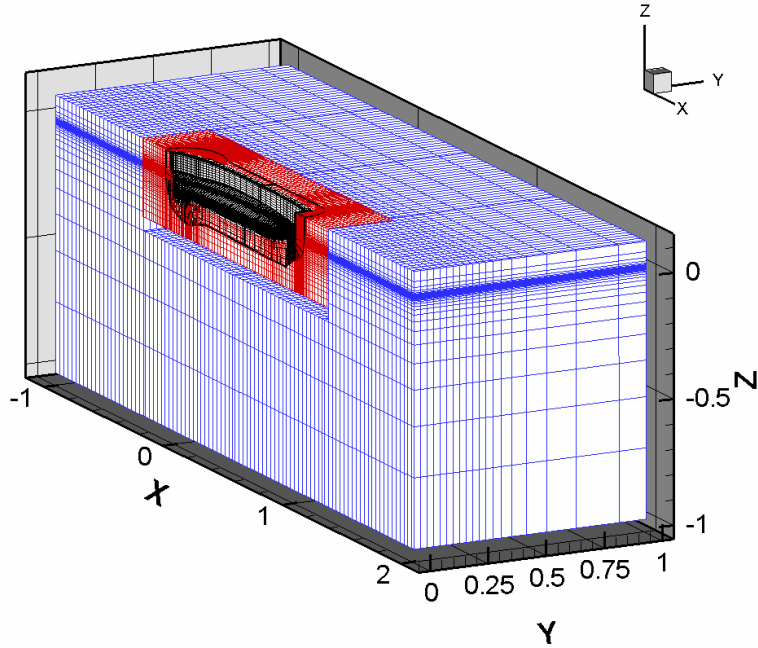


Figure 5: grid used for the wave diffraction problem.

The initial conditions are set for a sinusoidal progressive wave with amplitude $A = 0.006$, as in the experimental conditions. The boundary conditions are summarized in table 1.

	ϕ	p	k	ω	U	V	W
<i>inlet</i> ($x = -1$)	Eq. (40)	exact solution	$k_{fs} = 10^{-7}$	$\omega_{fs} = 9$	exact solution	$V = 0$	exact solution
<i>exit</i> ($x = 2$)	$\frac{\partial \phi}{\partial n} = 0$	$\frac{\partial p}{\partial n} = 0$	$\frac{\partial k}{\partial n} = 0$	$\frac{\partial \omega}{\partial n} = 0$	$\frac{\partial^2 U}{\partial n^2} = 0$	$\frac{\partial^2 V}{\partial n^2} = 0$	$\frac{\partial^2 W}{\partial n^2} = 0$
<i>far-field</i> ($y = 1$)	$\frac{\partial \phi}{\partial n} = 0$	$\frac{\partial p}{\partial n} = 0$	$\frac{\partial k}{\partial n} = 0$	$\frac{\partial \omega}{\partial n} = 0$	$\frac{\partial U}{\partial n} = 0$	$\frac{\partial V}{\partial n} = 0$	$\frac{\partial W}{\partial n} = 0$
<i>far-field</i> ($z = -1$)	$\frac{\partial \phi}{\partial n} = 1$	$\frac{\partial p}{\partial n} = 0$	$\frac{\partial k}{\partial n} = 0$	$\frac{\partial \omega}{\partial n} = 0$	$U = 1$	$V = 0$	$W = 0$
<i>symmetry</i> ($y = 0$)	$\frac{\partial \phi}{\partial n} = 0$	$\frac{\partial p}{\partial n} = 0$	$\frac{\partial k}{\partial n} = 0$	$\frac{\partial \omega}{\partial n} = 0$	$\frac{\partial U}{\partial n} = 0$	$V = 0$	$\frac{\partial W}{\partial n} = 0$
<i>far-field</i> ($z = 0.1$)	$\frac{\partial \phi}{\partial n} = -1$	not needed	$\frac{\partial k}{\partial n} = 0$	$\frac{\partial \omega}{\partial n} = 0$	$\frac{\partial U}{\partial n} = 0$	$\frac{\partial V}{\partial n} = 0$	$\frac{\partial W}{\partial n} = 0$
<i>no slip</i> (ship wall)	$\frac{\partial \phi}{\partial n} = 0$	Eq. (37)	$k = 0$	$\omega = \frac{60}{\text{Re } \beta y^{+2}}$	$U = 0$	$V = 0$	$W = 0$

Table 1: boundary conditions for the forward speed diffraction problem

The computation was started at $t = 0$, with sudden imposition of the initial and boundary

conditions, which causes an acceleration transient. The time step was chosen to be 0.00683, so that each wave period was discretized in 80 time steps. The initial transient is due to the time needed for the ship boundary layer to grow and for the Kelvin waves to develop, but an essentially periodic solution was achieved after about 3 non-dimensional time units, equivalent in our non dimensionalization to an advance of three ship lengths L . After the periodic solution was achieved, 5 more periods were run.

We will concentrate in this paper on comparisons with free surface elevations and wake velocities. We chose to compare against quarter periods at $t/T = 0, 1/4, 1/2$ and $3/4$. The phase is set in such a way that at the beginning of the period T the crest of the wave is coincident with the bow of the ship, $x = 0$. Since the wavelength is $\lambda = 1.5L$, the far-field crest will be located at $x = 0.375, 0.75$ and 1.125 for $t/T = 1/4, 1/2$ and $3/4$, respectively.

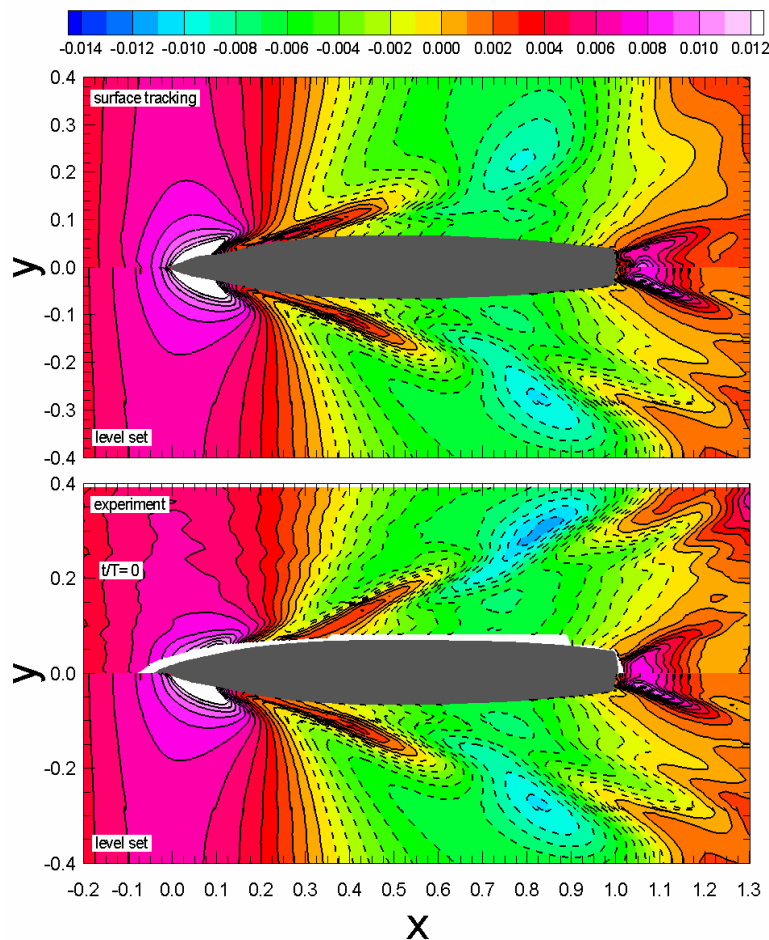


Figure 6: experimental, surface tracking and level-set free-surface solutions for $t/T=0$.

The free surface elevation predicted by the single-phase level-set method is compared against the experimental data and surface-tracking simulations⁷ for the periodic state at $t/T = 0$ in Fig. 6. The single-phase level set results show an excellent agreement with the

experimental data capturing appropriately the Kelvin waves and the near-hull features of the free surface. Compared to the surface-tracking results, the single-phase level set shows much better agreement with the experimental data. The surface-tracking computations were made on a coarser grid (750,000 grid points), which could partially account for the poorer results. Notice, however, that the implementation of overset grids with surface tracking methods would be complicated and expensive, since the interpolation coefficients would need to be recomputed every time the grid moves, several times per time step, at every time step in an unsteady problem. Thus, in surface capturing methods much better quality grids can be used.

Fig. 7 shows the elevations from the experimental data and the level set computations for the other three quarter periods: $t/T = 1/4, 1/2$ and $3/4$. Again, excellent agreement with the experimental data is evident, though the elevation gradients appear to be slightly smoothed, resulting in some underprediction of the crests and troughs on the Kelvin wave. Contrarily, the wave elevation on the stern is slightly overpredicted.

6 CONCLUSIONS

An unsteady single-phase level-set method has been presented. The method relies on the level set function to detect the interface, and on velocity extensions and pressure interpolations to enforce the jump conditions at the interface. The computation of the time derivatives to properly evaluate the total derivatives is discussed in detail. The method is tested against three unsteady cases: an inviscid linear progressive wave, the viscous sloshing in a two-dimensional tank and the flow around a surface ship under regular head waves. In the three cases the method has performed very well compared to either analytical or experimental results.

The presented method has several potential advantages against the standard two-phase level set method, and of course some disadvantages. One of the advantages is that the computation takes place only in water, with potential important savings computing simpler equations in air. In addition, the computation is performed in a fluid with constant properties, avoiding the problem related with large density ratios in two-phase level set methods. Since the jump conditions are imposed explicitly, no transition zone appears. As for the shortcomings, the method does not solve the fluid equations in air and therefore no problems in which air entrapment occurs can be solved. In addition, the stresses on the liquid caused by the air must be negligible or specified somehow.

In principle any problem that is not restricted by the limitations previously stated can be tackled with the unsteady single-phase level-set method. This includes surface-piercing bodies with large-amplitude waves or motions, steep waves, etc. Linear and nonlinear problems can be solved since we retain the nonlinear terms on the equations and on the jump conditions.

7 ACKNOWLEDGEMENTS

This research was sponsored by the Office of Naval Research under Grant N00014-01-1-0073, with Dr. Patrick Purtell as the program manager.

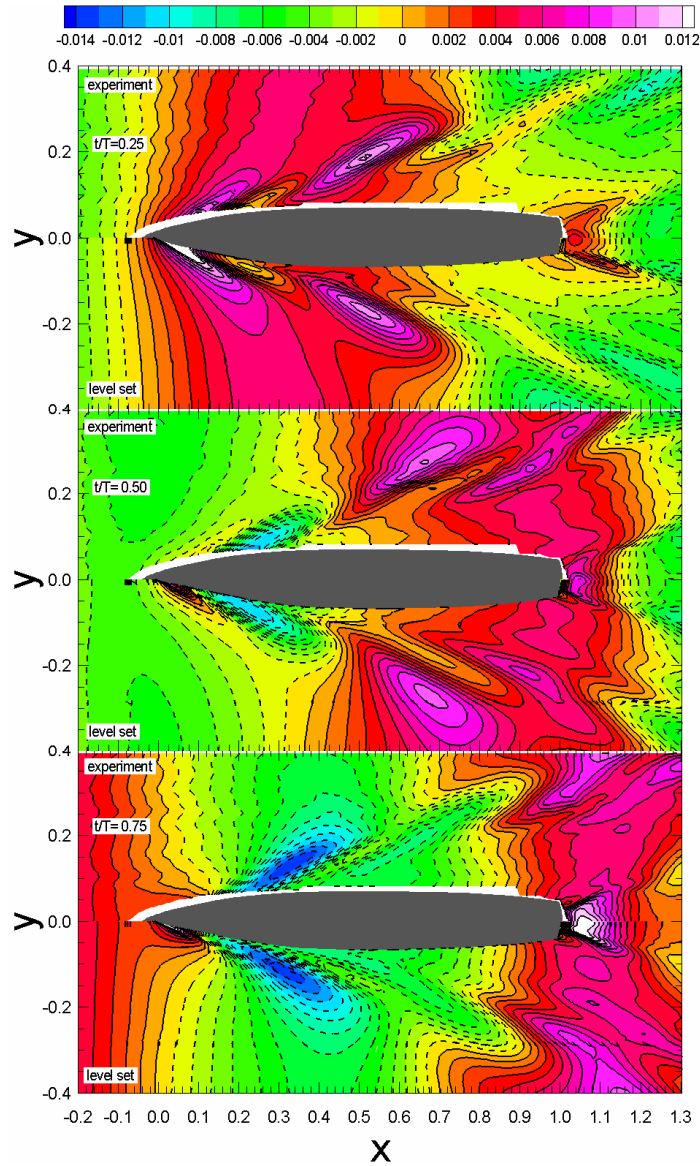


Figure 7: experimental and level-set free-surface solutions for $t/T=0.25, 0.5$ and 0.75 .

8 REFERENCES

1. J. A. Sethian and P. Smereka, Level set Methods for Fluid Interfaces, *Annu. Rev. Fluid Mech.* **35**, 341-372 (2003)
2. S. J. Osher and J. A. Sethian, Front Propagating with Curvature Dependent Speed: Algorithms Based on Hamilton-Jacobi Formulations, *J. Comput. Phys.* **79**, 12-49 (1988)
3. S. J. Osher and R. P. Fedkiw, Level set Methods: an Overview and Some Recent Results, *J. Comput. Phys.* **169**, 463-502 (2001)

4. M. S. Kim and W. I. Lee, A New VOF-Based Numerical Scheme for the Simulation of Fluid Flow with Free Surface. Part I: New Free Surface-Tracking Algorithm and its Verification, *Int. J. Num. Meth. Fluids* **42**, 765-790 (2003)
5. R. Wilson, F. Stern, H. Coleman and E. Paterson, Comprehensive Approach to Verification and Validation of CFD Simulations-Part 2: Application for RANS Simulation of a Cargo/Container Ship, *ASME J. Fluids Eng.* **123**, 803-810 (2001)
6. C. O. E. Burg, K. Sreenivas, and D. G. Hyams, Unstructured Nonlinear Free Surface Simulations for the Fully-Appended DTMB Model 5415 Series Hull Including Rotating Propulsors, *24th ONR Symp. on Naval Hydrodynamics*, Fukuoka, Japan (2002)
7. R. V. Wilson and F. Stern, Unsteady CFD Method for Naval Combatants in Waves, *22nd ONR Symp. on Naval Hydrodynamics*, Washington DC, USA (1998)
8. S. H. Rhee and F. Stern, Unsteady RANS Method for Surface Ship Boundary Layer and Wake and Wave Field, *Int. J. Num. Meth. Fluids* **37**, 445-478 (2001)
9. R. V. Wilson, P. M. Carrica and F. Stern, Unsteady RANS Simulation of a Surface Combatant with Roll Motion, submitted to *Comp. Fluids* (2004)
10. G. Weymouth, R. V. Wilson and Stern, RANS CFD Predictions of Pitch and Heave Ship Motions in Head Seas, accepted for publication in *J. Ship Res.* (2004)
11. L. Larsson, F. Stern and V. Bertram, Benchmarking of Computational Fluid Dynamics for Ship Flows: The Gothenburg 2000 Workshop, *J. Ship Res.* **47**, 63-81 (2003)
12. C. W. Hirt and B. D. Nichols, Volume of Fluid (VOF) Method for Dynamics of Free Boundaries, *J. Comput. Phys.* **39**, 201-221 (1981)
13. S. O. Unverdi and G. Tryggvason, A Front Tracking Method for Viscous, Incompressible, Multi-Fluid Flows, *J. Comput. Phys.* **100**, 25-37 (1992)
14. R. Azcueta, S. Muzaferija and M. Peric, Computation of Breaking Bow Waves For a Very Full Hull Ship, *7th Int. Conf. Numerical Ship Hydrodynamics*, Nantes, France (1999)
15. Y. Sato, H. Miyata and T. Sato, CFD Simulation of 3-Dimensional Motion of a Ship in Waves: Application to an Advancing Ship in Regular Heading Waves, *J. Marine Sci. Tech.* **4**, 108-116 (1999)
16. M. Vogt and L. Larsson, Level set Methods for Predicting Viscous Free Surface Flows, *7th Int. Conf. Numerical Ship Hydrodynamics*, Nantes, France (1999)
17. A. Cura Hochbaum and C. Shumann, Free Surface Viscous Flow Around Ship Models, *7th Int. Conf. Numerical Ship Hydrodynamics*, Nantes, France (1999)
18. A. Cura Hochbaum and M. Vogt, Flow and Resistance Prediction for a Container Ship, *Proc. Gothenburg 2000, A Workshop on CFD in Ship Hydrodynamics*, Gothenburg, Sweden (2000)
19. A. Cura Hochbaum and M. Vogt, Towards the Simulation of Seakeeping and Maneuvering Based on the Computation of the Free Surface Viscous Ship Flow, *24th ONR Symp. on Naval Hydrodynamics*, Fukuoka, Japan (2002)
20. A. Di Mascio, R. Broglia & R. Muscari, A Single-Phase Level set Method for Solving

- Viscous Free Surface Flows, submitted to *Int. J. Num. Meth. Fluids* (2004)
21. M. Sussman, P. Smereka and S. J. Osher, A Level set Approach to Computing Solutions to Incompressible Two-Phase Flow, *J. Comput. Phys.* **114**, 146-159 (1994).
 22. D. A. Drew and S. L. Passman, *Theory of Multicomponent Fluids*, Springer-Verlag, New York, p. 89 (1998)
 23. C. Marangoni, Ueber die Ausbreitung der Tropfen einer Flüssigkeit auf der Oberfläche einer Anderen, *Ann. Phys. Chem.* **143**, 337-354 (1871)
 24. J. U. Brackbill, D. B. Kothe and C. A. Zemach, A Continuum Method for Modeling Surface Tension, *J. Comput. Phys.* **100**, 335-354 (1992)
 25. R. P. Fedkiw, T. Aslam, B. Merriman and S. J. Osher, A non-Oscillatory Eulerian Approach to Interfaces in Multimaterial Flows (the Ghost Fluid Method), *J. Comput. Phys.* **154**, 393-427 (1999)
 26. M. Kang, R. P. Fedkiw and L. D. Liu, A Boundary Condition Capturing Method for Multiphase Incompressible Flow, *J. Sci. Comp.* **15**, 323-360 (2000)
 27. F. R. Menter, Two-Equation Eddy Viscosity Turbulence Models for Engineering Applications, *AIAA J.* **32**, 1598-1605 (1994)
 28. P. M. Carrica, R. Wilson & F. Stern, An Unsteady Single-Phase Level Set Method for Viscous Free Surface Flows, submitted to *Int. J. Num. Meth. Fluids* (2004)
 29. D. Adalsteinsson and J. A. Sethian, The Fast Construction of Extension Velocities in Level Set Methods, *J. Comput. Phys.* **148**, 2-22 (1999)
 30. E. G. Paterson, R. V. Wilson and F. Stern, General-Purpose Parallel Unsteady RANS Ship Hydrodynamics Code: CFDShip-Iowa, *IIHR report 432*, Iowa Institute of Hydraulic Research, The University of Iowa (2003).
 31. R. Wilson, P. M. Carrica and F. Stern, Steady and Unsteady Single-Phase Level-Set Method for Large Amplitude Ship Motions and Maneuvering, to be presented at 25th *ONR Symp. on Naval Hydrodynamics*, New Foundland, Canada (2004)
 32. G. X. Wu, R. Eatock Taylor and D. M. Greaves, The Effect of Viscosity on the Transient Free Surface Waves in a Two-Dimensional Tank, *J. Eng. Math* **40**, 77-90 (2001)
 33. R. Eatock Taylor, A. G. L. Borthwick, M. J. Chern and G. Zhu, Modelling Unsteady Viscous Free Surface Flows, *Int. Maritime Res. & Tech. Conf.*, Crete, Greece (2001)
 34. L. Gui, J. Longo, B. Metcalf, J. Shao and F. Stern. Forces, Moment and Wave Pattern for Surface Combatant in Regular Head Waves. Part I: Measurement systems and uncertainty analysis, *Exp. Fluids* **31**, 674-680 (2002)
 35. L. Gui, J. Longo, B. Metcalf, J. Shao and F. Stern. Forces, Moment and Wave Pattern for Surface Combatant in Regular Head Waves. Part I: Measurement results and discussion, *Exp. Fluids* **32**, 27-36 (2002)
 36. J. Longo, J. Shao, M. Irvine and F. Stern. Phase-Averaged PIV for Surface Combatant in Regular Head Waves, 24th *ONR Symp. on Naval Hydrodynamics*, Fukuoka, Japan (2002)
 37. N. E. Suhs, S. E. Rogers and W. E. Dietz, Pegasus 5: An Automated Pre-Processor for Overset-Grid CFD, *AIAA paper 2002-3186*, 32nd *AIAA Fluid Dynamics Conf.*, St. Louis (2002)